

Josephson (001) tilt grain boundary junctions of high temperature superconductors

Gerald B. Arnold^{1,*} and Richard A. Klemm^{2,†}

¹*Department of Physics, University of Notre Dame, Notre Dame, IN*

²*Department of Physics, Kansas State University, Manhattan, KS 66506*

(Dated: November 3, 2004)

We calculate the critical current I_c across in-plane (001) tilt grain boundary junctions of high temperature superconductors. We solve for the hole-doped tight-binding electronic states in each half-space, and weakly connect the two half-spaces by either specular or random Josephson tunneling. We treat both symmetric and fully asymmetric junctions with s -, extended- s , or $d_{x^2-y^2}$ -wave order parameters. Many $d_{x^2-y^2}$ -wave results are in qualitative disagreement with the analogous Sigrist-Rice forms used extensively to interpret “phase-sensitive” experiments.

PACS numbers: 74.20.Rp, 74.50.+r, 74.78.Bz

Because of its relation to the mechanism for superconductivity in the high temperature superconducting compounds (HTSC), there has long been a raging debate regarding their orbital symmetry of the superconducting order parameter (OP).^{1,2,3,4} Only “phase-sensitive” experiments involving Josephson tunneling can distinguish the OP from the non-superconducting pseudogap.^{1,4,5} Although the first in-plane phase-sensitive experiment on $\text{YBa}_2\text{Cu}_3\text{O}_{7-\delta}$ (YBCO) suggested a dominant s -wave OP,⁶ experiments using tricrystal films of YBCO, $\text{Bi}_2\text{Sr}_2\text{CaCu}_2\text{O}_{8+\delta}$ (Bi2212), and $\text{Nd}_{1.85}\text{Ce}_{0.15}\text{CuO}_{4+\delta}$ (NCCO), and tetracrystal films of YBCO and $\text{La}_{2-x}\text{Ce}_x\text{CuO}_{4-y}$ suggested that these materials had a dominant $d_{x^2-y^2}$ -wave OP.^{1,7,8,9,10,11}

Very different results were obtained for c -axis junctions. Low temperature T c -axis Josephson junctions between Pb and YBCO, Bi2212, and NCCO suggested varying amounts of an s -wave OP component.^{12,13,14,15} More recently, three Bi2212 c -axis twist Josephson junction experiments showed that the OP has at least a substantial, and possibly a dominant s -wave component for T up to the transition temperature T_c .^{4,16,17,18,19} Here we investigate if there might be a theoretical, as well as an extrinsic, reason for these qualitatively different results.⁴

To date, the only theoretical treatments of in-plane (001) tilt GB junctions have used either the simplistic Ginzburg-Landau (GL) treatment,²⁰ or made the assumptions that the in-plane Fermi surface (FS) had a circular cross-section, and that neither the FS-restricted $d_{x^2-y^2}$ -wave OP $\propto \cos(2\phi_{\mathbf{k}})$ nor the FS details differed on the junction interfaces from their bulk values.²¹ Here we explicitly take account of the tight-binding hole FS observed using angle resolved photoemission spectroscopy and of the surface boundary conditions (BC’s) at the interfaces. We find that a $d_{x^2-y^2}$ -wave OP can be consistent with the tricrystal experiments, but not for specular GB tunneling, implying that defects play an essential role in the experiments.¹ An important modification to the tetracrystal experiment is also warranted.²

We let θ_i for $i = L, R$ be the angles the x_i axes on the left (L) and right (R) sides make with the normal to a straight GB interface, Fig. 1. GL treatments of the Josephson current I for a $d_{x^2-y^2}$ -wave OP yielded for

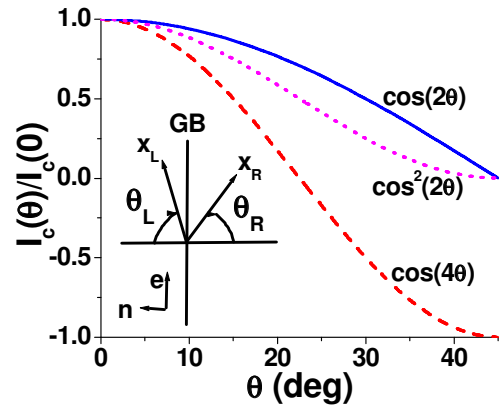


FIG. 1: Plots of $I_c(\theta)/I_c(0)$ for symmetric and asymmetric junctions with a $d_{x^2-y^2}$ -wave OP in the straight and faceted GL models. Inset: Sketch of a (001) tilt GB junction.

straight and faceted GB’s,^{7,20}

$$I_d^{st} = I_{cd}^{st} \cos(2\theta_L) \cos(2\theta_R) \sin(\delta\phi), \quad (1)$$

$$I_d^f = I_{cd}^{st} \cos[2(\theta_L + \theta_R)] \sin(\delta\phi)/2, \quad (2)$$

where $\delta\phi = \phi_L - \phi_R$ is the OP phase difference across the GB. These have the form $I = I_0 \sin(\delta\phi)$, where the critical current $I_c = |I_0|$. $I_0 > 0$ and $I < 0$ are the “0-” and “ π -junction” cases, as $I = I_c \sin(\delta\phi + \pi)$ in the latter. For asymmetric junctions, $\theta_L = \theta, \theta_R = 0$, $I_d^{st,f}(\theta)/I_d^{st,f}(0) = \cos(2\theta)$. For symmetric junctions, $\theta_L = \theta_R = \theta$, $I_d^{st,f}(\theta)/I_d^{st,f}(0) = \cos^2(2\theta), \cos(4\theta)$, respectively. These GL results shown in Fig. 1 differ qualitatively from our microscopic results for HTSC.

To calculate I across an in-plane GB, we modify our previous technique for c -axis tunneling.²² We assume the Fourier transform of the quasiparticle Green function matrix in the bulk of the i th superconductor is

$$\hat{G}(\mathbf{k}^i, \omega) = -\frac{i\omega + \Delta(\mathbf{k}^i)\tau_1 + \xi(\mathbf{k}^i)\tau_3}{\omega^2 + |\Delta(\mathbf{k}^i)|^2 + \xi^2(\mathbf{k}^i)}, \quad (3)$$

$$\xi_0(\mathbf{k}^i) = -J_{||}[\cos(k_x^i a) + \cos(k_y^i a)]$$

$$-\nu \cos(k_x^i a) \cos(k_y^i a) - \mu], \quad (4)$$

where ω is a Matsubara frequency, \mathbf{k}^i is the wave vector on the i th GB side, $\Delta(\mathbf{k}^i)$ is the respective two-dimensional (2D) gap function, a is the tetragonal in-plane lattice constant, J_{\parallel} , μ and ν are parameters defining the chemical potential and in-plane dispersion, respectively, and τ_j are the Pauli matrices. We take $\xi(\mathbf{k}^i) = \xi_0(\mathbf{k}^i) + J_{\perp}[1 - \cos(k_z^i s)]$, where s is the c -axis repeat distance. Here we are mainly interested in the two-dimensional (2D) limit $J_{\perp} = 0$. For the tight-binding FS appropriate for Bi2212, FS2, we take $J_{\parallel} = 500$ meV, $\mu = 0.6$, and $\nu = 1.3$, and set $\xi_0(\mathbf{k}_F^i) = 0.22$ Å. A nearly circular FS, FS3, is obtained with $\mu = 1.0$ and $\nu = 0.22$.

Next, we construct the half-space Green function matrices on the i th side of a straight (001) tilt GB. We let $\hat{\mathbf{n}}$ and $\hat{\mathbf{e}}$ be unit vectors normal and parallel to the GB satisfying $\hat{\mathbf{e}} \times \hat{\mathbf{n}} = \hat{\mathbf{z}}$, as sketched in Fig. 1. Letting $k_{\parallel}^i = \mathbf{k}_i \cdot \hat{\mathbf{e}}$ and $k_{\perp}^i = \mathbf{k}_i \cdot \hat{\mathbf{n}}$, we set $\mathbf{k}_{\parallel}^i = (k_{\parallel}^i, k_z^i)$, $k_x^i = k_{\perp}^i \cos \theta_i - k_{\parallel}^i \sin \theta_i$, and $k_y^i = k_{\perp}^i \sin \theta_i + k_{\parallel}^i \cos \theta_i$. The lack of translational invariance requires a discrete indexing of the lattice planes along $\hat{\mathbf{n}}$. Thus, for integers n, m ,

$$\hat{G}_{m-n}(\mathbf{k}_{\parallel}^i, \omega) = \int_{-\pi/a_{\perp}^i}^{\pi/a_{\perp}^i} \frac{a_{\perp}^i dk_{\perp}^i}{2\pi} e^{ik_{\perp}^i a_{\perp}^i (m-n)} \hat{G}(\mathbf{k}^i, \omega),$$

where $\mathbf{k}_{\parallel}^i = (k_{\parallel}^i, k_z^i)$ and the $a_{\perp}^i/a = \min(\cos \theta_i, \sin \theta_i)$ for $90^\circ > \theta_i > 0^\circ$, $a_{\perp}^i = a$ for $\theta_i = 0^\circ, 90^\circ$ are the respective lattice plane separations along $\hat{\mathbf{n}}$. We choose the GB interface between lattice planes 1 and 0 and set $n, m \geq 1$, $n, m \leq 0$ for $i = R, L$, respectively. Suppressing the \mathbf{k}_{\parallel}^i and ω dependencies, we construct each surface \hat{g}_{nm} from a combination of the \hat{G}_{mn} that obeys the free surface boundary conditions (BC's) $\hat{g}_{m0} = \hat{g}_{0n} = 0$ for $n, m \geq 1$ and $\hat{g}_{m1} = \hat{g}_{1n} = 0$ for $n, m \leq 0$, obtaining^{22,23}

$$\hat{g}_{mn} = \hat{G}_{|m-n|} - \hat{G}_{m+n}, \quad \text{for } m, n \geq 1, \quad (5)$$

$$\hat{g}_{mn} = \hat{G}_{|m-n|} - \hat{G}_{2-m-n}, \quad \text{for } m, n \leq 0. \quad (6)$$

We then paste together the two half-space layered superconductors. We set $\Delta(\mathbf{k}^i) = \exp(i\phi_i) \text{Re}\Delta(\mathbf{k}^i)$ and define \overline{g}_{nm}^{pq} to be the (pq) th matrix element of the rank 2 matrix \hat{g}_{nm} with $\phi_i = 0$. To leading order in the general tunneling matrix element $J_J(\mathbf{k}_{\parallel}^L, \mathbf{k}_{\parallel}^R)$, we obtain

$$I = \frac{4eT}{A^2} \sum_{\mathbf{k}_{\parallel}^R, \mathbf{k}_{\parallel}^L, \omega} |J_J(\mathbf{k}_{\parallel}^L, \mathbf{k}_{\parallel}^R)|^2 \overline{g}_{11}^{12}(\mathbf{k}_{\parallel}^R, \omega) \times \overline{g}_{00}^{21}(\mathbf{k}_{\parallel}^L, \omega) \sin(\delta\phi), \quad (7)$$

where A is the junction area, e is the electron charge, $\delta\phi = \phi_L - \phi_R$, $-\pi/s \leq k_z^i \leq \pi/s$, $-\pi/a_{\parallel}^i \leq k_{\parallel}^i \leq \pi/a_{\parallel}^i$, and the $a_{\parallel}^i = a^2/a_{\perp}^i$ are the lattice constants along $\hat{\mathbf{e}}$.

Experimentally for large misalignment angles $\theta > 20^\circ$, $I_c(\theta) \ll I_c(0)$,² justifying this weak tunneling assumption, although the approximation is less accurate for

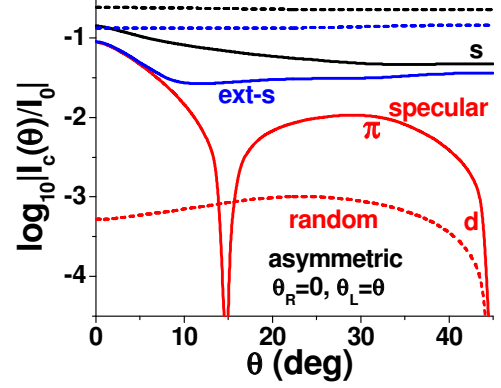


FIG. 2: Plots of $\log_{10} |I_c(\theta)/I_0|$ for asymmetric junctions with $\theta_R = 0, \theta_L = \theta$, for s - (black), extended- s - (blue), and $d_{x^2-y^2}$ -wave (red) superconductors, for specular (solid) and random (dashed) tunneling. The d -wave curves satisfy $I_c(45^\circ - \theta) = -I_c(\theta)$, but the s - and extended- s -wave curves satisfy $I_c(45^\circ - \theta) = I_c(\theta)$.

small θ . Since the effects induced by the GB to the real-space $d_{x^2-y^2}$ -wave pairing interaction are formidable, here we only treat the surface BC effects, and discuss the effects of self-consistency elsewhere.²⁴ We include the limiting cases of specular (or coherent) tunneling, where $\mathbf{k}_{\parallel}^R = \mathbf{k}_{\parallel}^L$, and random (or incoherent) tunneling, where \mathbf{k}_{\parallel}^R and \mathbf{k}_{\parallel}^L are independent, writing²⁵

$$|J_J(\mathbf{k}_{\parallel}^L, \mathbf{k}_{\parallel}^R)|^2 = |J_J^{\text{sp}}|^2 \delta_{\mathbf{k}_{\parallel}^R, \mathbf{k}_{\parallel}^L} A + |J_J^{\text{r}}|^2. \quad (8)$$

Since lattices on opposite sides of straight (001) tilt GB junctions are generally incommensurate, random tunneling processes are important. Faceting and other imperfections provide additional random processes.^{26,27,28}

In Fig. 2, we present our results obtained from Eq. (7) for the low- T I_c across asymmetric junctions, $\theta_R = 0, \theta_L = \theta$, including the tight-binding FS2 and the surface BC effects. In this case, we assumed the $d_{x^2-y^2}$ - and extended- s -wave OP's to have the bulk real-space pairing forms $\Delta_0(T)[\cos(k_x^i a) - \cos(k_y^i a)]$ and $\Delta_0(T)|\cos(k_x^i a) - \cos(k_y^i a)|$, respectively. The ordinary- s -wave OP is $\Delta_0(T)$, independent of \mathbf{k}^i .²² We take $\Delta_0(0) = 10$ meV in our calculations, which implies a maximum d -wave OP of 20 meV. In Fig. 2, we plotted $\log_{10} |I_c(\theta)/I_0|$, where $I_0 = 4e|J_J^{\text{sp}}|^2/[a^3 s \Delta_0^2(0)]$, $4e|J_J^{\text{r}}|^2/[a^4 s^2 \Delta_0^2(0)]$, respectively.²⁵ The dashed (solid) curves are the results for specular (random) tunneling, respectively. The specular junction behaves as a π -junction only for $14.9^\circ \leq \theta \leq 45^\circ$ and $75.1^\circ \leq \theta \leq 90^\circ$. We also investigated the role of J_{\perp} for the d -wave case. For random GB tunneling, as J_{\perp} increases to 40 meV, the broad peak in $I_c(\theta)$ becomes much flatter, and for much larger J_{\perp} , $I_c(\theta)$ non-monotonically approaches the GL result $\propto \cos(2\theta)$. For specular tunneling, $J_{\perp} = 10$ meV yields d -wave results nearly identi-

cal to those pictured for $J_{\perp} = 0$. Increasing J_{\perp} beyond $J_{\perp 0} \approx 40$ meV eliminates the regions for $0 \leq \theta \leq 45^{\circ}$ of π -junctions, so that the overall region of π -junctions are for $45^{\circ} \leq \theta \leq 90^{\circ}$, as for the GL case. Hence, for $J_{\perp} \leq J_{\perp 0}$, the specular, tight-binding asymmetric GB d -wave results are qualitatively different than the GL ones.

In Fig. 3, we present the analogous results for symmetric junctions. In this case, the specular d -wave junction behaves as a π -junction for $39.4^{\circ} \leq \theta \leq 50.6^{\circ}$, but is a 0-junction otherwise. For random tunneling, the symmetric d -wave junction behaves similarly to the straight GL model, Eq. (1), as both have $I_c(45^{\circ}) = 0$ but never behave as π -junctions. However, the d -wave GL facet model, Eq. (2), has $I_d^f(45^{\circ}) = -I_d^f(0^{\circ})$, which is qualitatively different.⁷ We note from Figs. 2, 3 that for small angle ($0 \leq \theta \leq 5^{\circ}$), specular junctions, the extended- s and $d_{x^2-y^2}$ -wave OP's lead to indistinguishable $I_c(\theta)$. However, for random tunneling, the d -wave $I_c(\theta)$ is much smaller than the extended- s -wave $I_c(\theta)$.

In Fig. 4 we compare our specular $I_c(\theta)/I_c(0)$ d -wave results with the surface BC's with those obtained from the bulk Green functions. We compare those results obtained with the tight-binding FS2 for asymmetric (Fig. 2) and symmetric (Fig. 3) junctions, and also our results for symmetric junctions obtained with the nearly circular FS3. For both symmetric GB cases, there are no regions in $0^{\circ} \leq \theta \leq 45^{\circ}$ of π -junctions for the bulk calculations. Including the surface effects, these symmetric GB cases have π -junctions for $39.4^{\circ} \leq \theta \leq 50.6^{\circ}$ and $29.2^{\circ} \leq \theta \leq 55.8^{\circ}$ for FS2 and FS3, respectively. For asymmetric junctions with FS2, the bulk calculation leads to weak π -junctions for $23.7^{\circ} \leq \theta \leq 28.3^{\circ}$ with a negative slope at 45° , yielding additional π -junctions for $45^{\circ} \leq \theta \leq 61.7^{\circ}$ and $66.3^{\circ} \leq \theta \leq 90^{\circ}$. The surface BC's greatly enhance the magnitude and range of such π -junctions to $14.9^{\circ} \leq \theta \leq 45^{\circ}$ and $75.1^{\circ} \leq \theta \leq 90^{\circ}$, and change the sign of the slope at 45° . Thus, we conclude that the surface BC effects cannot be ignored, and the GL d -wave models for straight and faceted junctions are qualitatively incorrect for FS2.²⁰

We remark that the ordinary- s - and extended- s -wave OP's lead to $I_c(0)$ values that are comparable to each other for both tunneling mechanisms. However, for the $d_{x^2-y^2}$ -wave OP, random tunneling leads to a suppression of $I_c(0)$ by a factor of 461 from that of the ordinary- s -wave OP. This suggests that $I_c(0)$ for the $d_{x^2-y^2}$ -wave OP with weak, random tunneling is unlikely to be consistent with the large values observed experimentally across low-angle (001) tilt junctions.² The broad peak in $I_c(\theta)$ for the d -wave OP with random tunneling for both asymmetric and symmetric is also inconsistent with most experimental data. On the other hand, the d -wave OP with specular tunneling does show a rapid decrease in $I_c(\theta)/I_c(0)$ with increasing θ , in agreement with low-angle experiments,² but vanishes at 14.9° and 39.4° , respectively, unlike the experiments.²

We also calculated $I_c(\theta)$ at low T across GB's with the nearly circular FS3. For asymmetric GB's, our d -wave

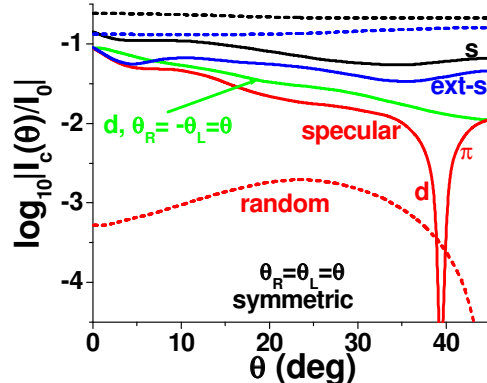


FIG. 3: Plots of $\log_{10} |I_c(\theta)/I_0|$ for symmetric junctions with $\theta_U = \theta_L = \theta$, for s -, extended- s -, and $d_{x^2-y^2}$ -wave superconductors. Also shown is the specular d -wave curve (solid green) for $\theta_R = -\theta_L = \theta$. All curves satisfy $I_c(45^{\circ} - \theta) = I_c(\theta)$.

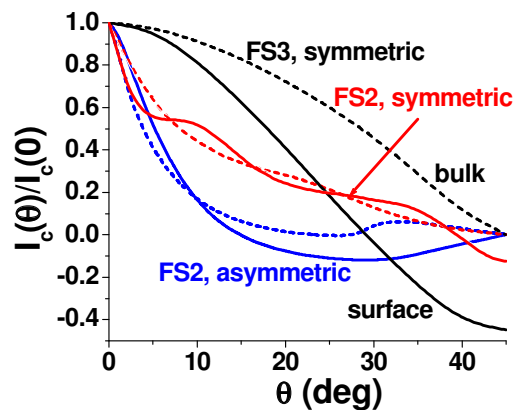


FIG. 4: Plots of $I_c(\theta)/I_c(0)$ for the $d_{x^2-y^2}$ -wave OP with specular tunneling, with (solid) and without (dashed) the surface boundary conditions, for symmetric GB junctions with FS2 (red) and FS3 (black), and for asymmetric GB junctions with FS2 (blue).

results agree with the GL model, $I_c(\theta)/I_c(0) \approx \cos(2\theta)$, for both specular and random tunneling, but for the latter, $I_c(0)$ nearly vanishes for a d -wave OP. For symmetric GB's, with random tunneling, $I_c(\theta)/I_c(0) \approx \cos^2(2\theta)$, as in the GL model for straight symmetric junctions (Fig. 1).

Tricrystal experiments were performed for a variety of hole-doped superconductors.^{1,7,8} Tricrystal (a) consists of one asymmetric $0^{\circ}/60^{\circ}$ junction and two $0^{\circ}/30^{\circ}$ junctions. Tricrystal (b) consists of two $0^{\circ}/71.6^{\circ}$ junctions and one symmetric $18.4^{\circ}/18.4^{\circ}$ junction. Tricrystal (c) consists of two asymmetric $0^{\circ}/73^{\circ}$ junctions and an asymmetric $2^{\circ}/32^{\circ}$ junction.^{1,9} Assuming a predominant $d_{x^2-y^2}$ -wave OP,⁷ our results show that tricrystal

(a) would have two π -junctions if the tunneling were specular, and one π -junction if it were random. Tricrystal (b) should have no π -junctions, as claimed. Tricrystal (c), if the $2^\circ/32^\circ$ junction can be approximated by an asymmetric $0^\circ/34^\circ$ junction, would have one π -junction for specular tunneling, and two π -junctions for random tunneling. Since it was claimed that an odd number of π -junctions leading to a spontaneous half-integral flux quantum was observed only in tricrystal (a),^{1,9} our results are only consistent with those observations if the tunneling is non-specular.

Tetracrystals consisting of highly twinned thin films of YBCO and LCCO containing a symmetric $0^\circ/0^\circ$ junction and a $45^\circ/\pm 45^\circ$ junction, plus two symmetric $22.5^\circ/22.5^\circ$ junctions were made.^{10,11} For comparison, they also made bicrystals with two symmetric $22.5^\circ/22.5^\circ$ junctions. We also calculated the asymmetric case $\theta_R = -\theta_L = \theta$ for a $d_{x^2-y^2}$ -wave OP, and our results are presented in Fig. 3. Random tunneling leads to the same curve pictured for symmetric junctions. The case for specular tunneling including the surface BC's is shown by the green solid curve, and at 45° , is opposite in sign to the symmetric junction case. If the tunneling were non-specular, as required for the d -wave interpretation of the tricrystal experiments, then the $45^\circ/\pm 45^\circ$ junction would have the smallest (or vanishing, for random tunneling) J value for a d -wave OP. If instead the tunneling were specular, then that junction would allow a small but significant J value, but would behave either as a pi - or 0 -junction, respectively, for a d -wave OP. Thus, this tetracrystal would have an odd number of π -junctions

for specular tunneling and a d -wave OP, but no supercurrent for random tunneling. For a highly twinned thin film junction, both specular and random tunneling across the $45^\circ/\pm 45^\circ$ junction would lead to $J \approx 0$ for a $d_{x^2-y^2}$ -wave OP, contrary to the claims in the experiment.¹⁰ The other two junctions would not be π -junctions. Thus, the interpretation put forward by those authors should be re-examined, as the π -junction could arise extrinsically from defects in this very imperfect $45^\circ/\pm 45^\circ$ junction.^{10,11} We urge that the experiment be redesigned in the form of a tricrystal, omitting the $45^\circ/\pm 45^\circ$ junction.

In summary, we calculated the critical current I_c versus (001) in-plane tilt angle θ for symmetric and asymmetric grain boundary junctions, assuming the order parameter has either the s -, extended- s -, or $d_{x^2-y^2}$ -wave form. We used the Fermi surface appropriate for hole-doped cuprates, and took account of the surface boundary conditions appropriate for the interfaces. Our results differ qualitatively with those obtained from Ginzburg-Landau models,^{7,20} and indicate that the tricrystal experiments can only be understood for a $d_{x^2-y^2}$ -wave OP with non-specular tunneling. However, that interpretation is inconsistent with the tetracrystal experiments on similar materials, and leads to a $I_c(\theta)$ inconsistent with many experiments.² However, it has been suggested that the experimental $I_c(\theta)$ observed can only be understood in terms of interface defects, regardless of the OP.²⁷ Such defects may be the source of the observed π -junctions in the tricrystal and tetracrystal experiments, accounting for the apparent inconsistency between those and the c -axis bicrystal and cross-whisker experiments.^{4,16,17,19}

* Electronic address: garnold@nd.edu

† Electronic address: klemm@phys.ksu.edu

¹ C. C. Tsuei and J. R. Kirtley, Rev. Mod. Phys. **72**, 969 (2000).

² H. Hilgenkamp and J. Mannhart, Rev. Mod. Phys. **74**, 485 (2002).

³ K. A. Müller, Phil. Mag. Lett. **82**, 279 (2002).

⁴ R. A. Klemm, Int. J. Mod. Phys. B **12**, 2920 (1998); Phil. Mag. (in press).

⁵ R. A. Klemm in *Nonequilibrium Physics at Short Times Scales. Formation of Correlations*, edited by K. Morawetz (Springer, Berlin, 2004), pp. 381-400.

⁶ P. Chaudhari and S. Lin, Phys. Rev. Lett. **73**, 593 (1994).

⁷ C. C. Tsuei *et al.*, Phys. Rev. Lett. **73**, 593 (1994).

⁸ J. R. Kirtley *et al.*, Europhys. Lett. **36**, 707 (1996).

⁹ C. C. Tsuei and J. R. Kirtley, Phys. Rev. Lett. **85**, 182 (2000).

¹⁰ R. R. Schulz *et al.*, Appl. Phys. Lett. **76**, 912 (2000).

¹¹ B. Chesca *et al.*, Phys. Rev. Lett. **90**, 057004 (2003).

¹² A. G. Sun *et al.*, Phys. Rev. Lett. **72**, 2267 (1994); A. G. Sun *et al.*, Phys. Rev. B **54**, 6734 (1996).

¹³ R. Kleiner *et al.*, Phys. Rev. Lett. **76**, 2161 (1996).

¹⁴ M. Mößle and R. Kleiner, Phys. Rev. B **59**, 4486 (1999).

¹⁵ S. I. Woods *et al.*, IEEE Trans. Appl. Supercond. **9**, 3917 (1999).

¹⁶ Qiang Li *et al.*, Phys. Rev. Lett. **83**, 4160 (1999).

¹⁷ Y. Takano *et al.*, Physica C **408-410**, 296 (2004).

¹⁸ R. A. Klemm, Phys. Rev. B **67**, 174509 (2003).

¹⁹ Yu. I. Latyshev *et al.*, Phys. Rev. B **70**, 094517 (2004).

²⁰ M. Sigrist and T. M. Rice, J. Phys. Soc. Jpn. **61**, 4283 (1992).

²¹ Y. Tanaka and S. Kashiwaya, Phys. Rev. B **56**, 892 (1997).

²² G. B. Arnold and R. A. Klemm, Phys. Rev. B **62**, 661 (2000).

²³ S. H. Liu and R. A. Klemm, Phys. Rev. Lett. **73**, 1019 (1994).

²⁴ G. B. Arnold and R. A. Klemm, unpublished.

²⁵ R. A. Klemm *et al.*, Phys. Rev. B **58**, 14203 (1998).

²⁶ X. F. Zhang, D. J. Miller and J. Talvacchio, J. Mater. Res. **11**, 2440 (1996).

²⁷ A. Gurevich and E. A. Pashitskii, Phys. Rev. B **57**, 13878 (1998); *ibid.* **63**, 139901(E) (2001).

²⁸ K. M. Lang *et al.*, Nature (London) **415**, 412 (2002).